Edinburgh 2000-27
Dec 2000

Status of the LHCb Experiment[1]

Franz Muheim[2]
on behalf of the LHCb Collaboration
Department of Physics and Astronomy, The University of Edinburgh,
Mayfield Road, Edinburgh EH9 3JZ, Scotland/UK

Abstract

We present the status of the LHCb experiment which will make precision measurements of CP violation in B meson decays. The motivation for the experiment and an overview of the detector design are given. The vertex detector, ring imaging Cherenkov counter, calorimeters, and trigger systems are discussed in detail. We also present the expected physics performance for selected modes.

Presented at 7th International Conference on B-Physics at Hadron Machines, (BEAUTY2000), Sep 2000, Kibbutz Maagan, Israel.
Submitted to Nuclear Instruments and Methods A.

[1]This presentation is dedicated to Tom Ypsilantis, 1928 - 2000.
[2]E-mail: F.Muheim@ed.ac.uk

1 Introduction and Overview

CP Violation is one of the most outstanding puzzles in particle physics. More than third of a century after its discovery, CP violation still has only been observed in the neutral kaon system. In the Standard Model (SM) of particle physics the mixing of quarks is described by the Cabibbo-Kobayashi-Maskawa (CKM) matrix. For three generations of quarks and leptons, the CKM matrix has four free parameters, three Euler angles, and one complex phase. It is this phase which allows CP violation to occur within the SM. While CP violation in the kaon system is tiny and plagued by theoretical uncertainties the SM predicts large CP violating effects in the B meson system. This is illustrated by the two relevant unitarity conditions

$$\begin{aligned} V_{ud}V_{ub}^* + V_{cd}V_{cb}^* + V_{td}V_{tb}^* &= 0 \\ V_{tb}V_{ub}^* + V_{ts}V_{us}^* + V_{td}V_{ud}^* &= 0 \end{aligned}$$

which can be represented by unitarity triangles in the complex plane as shown in Figure 1. The lengths of the sides are all of the same order of magnitude. CP violating asymmetries correspond to non-zero values for the angles α, β, and γ. The relevant B decay channels are also indicated.

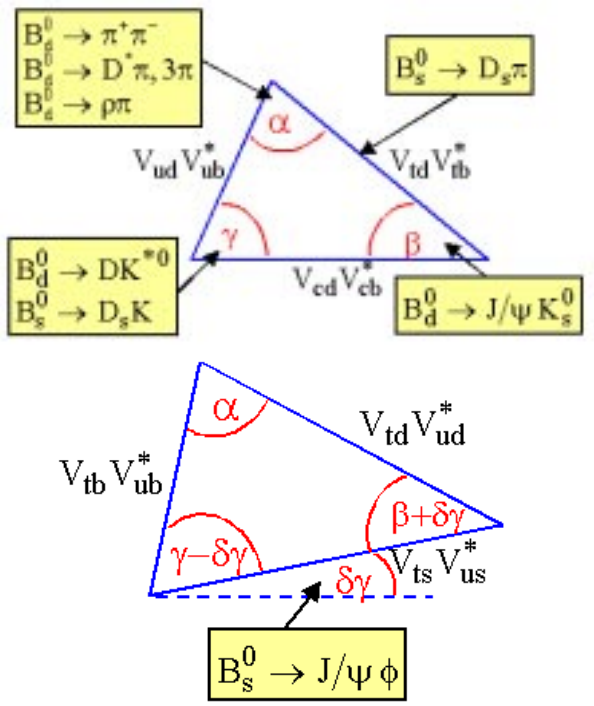

Figure 1: Two unitarity triangles. B decays and the angles and sides which they probe are also given.

However, we have no real understanding of CP violation. For example, baryogenesis tells us that beside the SM additional sources of CP violation are needed. For B mesons the SM makes accurate predictions in many decay channels which can be tested. Precise measurements of many CP violating angles overconstrain the unitarity triangles and allow to extract the parameters of the SM and of the possible new physics.

By 2005 the experiments BABAR, BELLE, CLEO-III, CDF, D0, and HERA-B will most likely have observed CP violation in the channel $B \to J/\psi K_S^0$ which determines the angle β. LHCb is a next generation experiment, starting in 2005 at the Large Hadron Collider (LHC). Given the large cross section of 500 μb the LHC will deliver 10^{12} $b\bar{b}$-quark pairs per year at a modest luminosity of $2 \times 10^{32}\mathrm{cm}^{-2}\mathrm{s}^{-1}$. All types of B mesons (B_d, B_u, B_s, B_c) will be produced. The LHCb experiment is designed to make precision measurements of CP violation in B mesons and to overconstrain the CKM matrix.

The LHCb detector shown in Figure 2 is a forward single arm spectrometer which exploits the fact that b and the $\bar{b}$ quark production angles are correlated and and that the production rates are strongly peaked forwards and backwards. The main challenges of the experiment are: i) the trigger which must select leptonic and hadronic final states, for example $B_d^0 \to \pi^+\pi^-$, out of the much more abundant background; ii) charged particle identification, i.e. the ability to distinguish between pions and kaons over a large momentum range and iii) an excellent proper time resolution for secondary vertices to separate B meson decays from light quark decays.

The detector design is as follows: A spectrometer magnet consisting of a normal conducting coil provides a bending power of $\int \mathrm{Bdl} = 4$ Tm with the field oriented vertically. The detector acceptance is ± 300 mrad (± 250 mrad) in the (non-) bending plane. Charged tracks are reconstructed in the inner and outer tracker. The inner tracker technology is either a triple-GEM gaseous or a silicon strip detector. The outer tracker consists of straw tube drift chambers, and is discussed in a separate

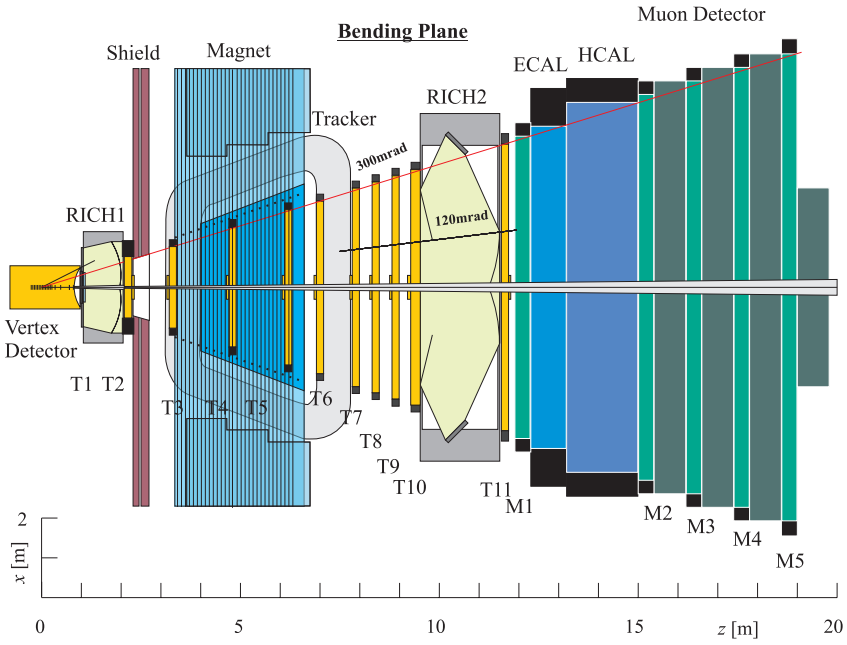

Figure 2: The LHCb spectrometer seen from above (bending plane).

contribution [1]. Wheels of silicon strip detectors are located around the interaction point for the reconstruction of primary and secondary vertices. Charged particle identification is provided by Ring Imaging Cherenkov (RICH) counters. The electromagnetic and hadronic calorimeters are used for triggering and shower reconstruction. The muon system is described in detail in another contribution [2]. The trigger is divided into four levels and the LHCb computing strategy is discussed in a separate contribution [3].

After the submission of the Technical Proposal [4] the LHCb experiment was approved in Sep 1998. Since then many major technology decision have been made. The Technical Design Report (TDR) for the Magnet has been approved in April 2000 [5] and very recently, in September 2000, the RICH and the Calorimeter subsystems have submitted their TDRs [6, 7].

2 Vertex Detector

The choice of technology for the LHCb vertex detector is single sided p-n or n-n silicon strip detectors with double metal read-out. The design of the vertex locator (VELO) is optimised for the Level-L1 trigger. Thus r and φ strip detectors alternate and the strip pitch varies such that the occupancy is roughly constant and below 0.5 %. The VELO wheels are split in halves and will be mounted onto radio frequency (RF) shields situated inside the vertex tank. During injection of beams into LHC the detector halves will be retracted by 3 cm which allows an active inner radius of 8 mm during physics runs. Depending on the actual radiation dose the detectors will be exposed to they may have to be replaced after a few years running of LHCb.

An optimisation of the VELO design has been carried out at the MAP simulation farm based on 300 Linux PCs [8] by generating, reconstructing, and analysing over 10 million events. The major changes of this improved VELO design are a "toblerone"-like shaped RF shield, an increase in the number of stations from 17 to 25 and 250 μm thick detectors with smaller pitch and radii. The design has an excellent proper time resolution of 43 ps for the decay $B_s^0 \rightarrow D_s^{\mp}\pi^{\pm}$ which corresponds to a sensitivity of up to $x_s \sim 75$ for $B_s^0\bar{B}_s^0$ oscillations. In addition, 9.5 hits per track are expected on average which allows for stand-alone tracking in the VELO.

Two designs for the front-end electronics are cur-

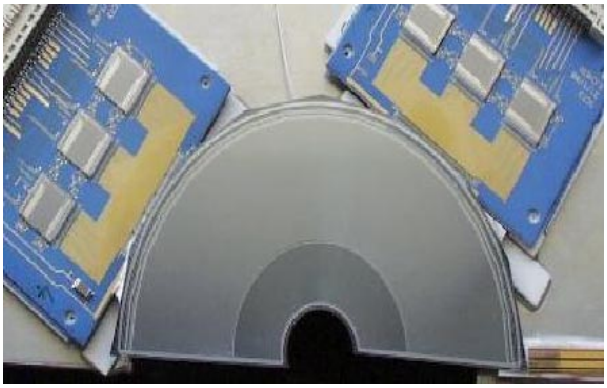

Figure 3: A silicon prototype detector equipped with LHC speed electronics.

rently under evaluation a) the SCTA128_VELO chip a prototype version of which has been used for testing the silicon detector and b) the BEETLE chip will be examined as soon as it becomes available. The design of a first prototype board of the off-detector electronics has been completed and tests are ongoing.

An extensive R&D programme to test the characteristics of the vertex detector is being carried out. Prototype silicon detectors equipped with LHC speed electronics, shown in Figure 3, have been successfully operated in beam tests at CERN. We have measured the signal shape, the spatial resolution and the cluster finding efficiency. Prototype detectors have also been heavily irradiated to simulate the expected radiation dose of more than three years of LHCb running. The performance before and after irradiation has been measured.

In summary the VELO design is well matched to the criteria important for vertexing in LHCb. The geometry with r and φ strips is optimum for the Level-L1 trigger. The pitch is smallest at the inner radius which improves upon the impact parameter resolution. The detectors are thin which minimises multiple scattering and the relatively low number of channels reflects in the cost of the system.

3 Ring Imaging Cherenkov Counters

The ability to distinguish between pions and kaons in various final states is a fundamental requirement of LHCb. In many important B-decay channels CP violation measurements are only possible with excellent hadron identification. For example, there are three kaons in the final state of the decay chain $B_s^0 \to D_s^{\mp} K^{\pm}$, $D_s^- \to \varphi\pi^-$, $\varphi \to K^+K^-$. The momentum spectrum of these tracks is quite broad extending beyond 100 GeV/c. Identifying kaons from the accompanying B hadron decay in the event of which a large fraction have momenta below $p < 10$ GeV/c also provides a valuable tag of the b quark production flavour. This means that the $\pi - K$ separation must span the range from $1\ \text{GeV/c} < p < 150\ \text{GeV/c}$.

This performance can only be achieved with RICH detectors. There is a strong correlation between the momentum and the polar angle of tracks, at wide angles the momentum spectrum is softer. Hence the RICH system is divided into two detectors shown schematically in Figure 4. An upstream detector (RICH 1) covers the full acceptance of LHCb. RICH 1 contains both a Silica aerogel radiator with $n = 1.03$ which is suitable for the lowest momentum tracks and a gaseous C_4F_{10} radiator well matched for the intermediate momentum region. A downstream detector (RICH 2) has a CF_4 radiator, to analyse high-momentum tracks. Its coverage is limited to the region 120 mrad (horizontal)×100 mrad (vertical). The three radiators are required to cover the full momentum range. In both detectors the Cherenkov

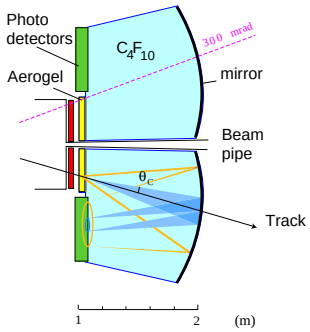

Figure 4: Layout of the RICH 1 and RICH 2 detectors. The production of two rings in the photo detectors is illustrated for RICH 1.

photons are focused by mirrors onto photo detector planes which are positioned outside the LHCb acceptance.

An intensive research and development programme has been undertaken for the LHCb RICH detectors. A major effort has been the development of the photo detector system, which must cover an area of 2.6m^2 with a large active area fraction at an acceptable cost. The RICH photo detectors must be sensitive to single photons with a peak quantum efficiency larger than 20 % and provide a spatial granularity of 2.5×2.5 mm^2. The read-out electronics for the photo detectors must be compatible with the LHC bunch crossing frequency (40 MHz) and the devices must work in an environment with large charged particle fluxes and fringe magnetic fields of up to 5 mT. Three options were investigated for the photo detectors: two based on hybrid photo diodes (HPD), the Pad HPD and the Pixel HPD; and the 64 channel Multianode Photo Multiplier Tube (MaPMT). A panel reviewed the three options and subsequently the Pixel HPD has been selected by the LHC collaboration as baseline photon detector. The MaPMT is kept as a backup option and the Pixel HPD must meet the performance criteria after one year.

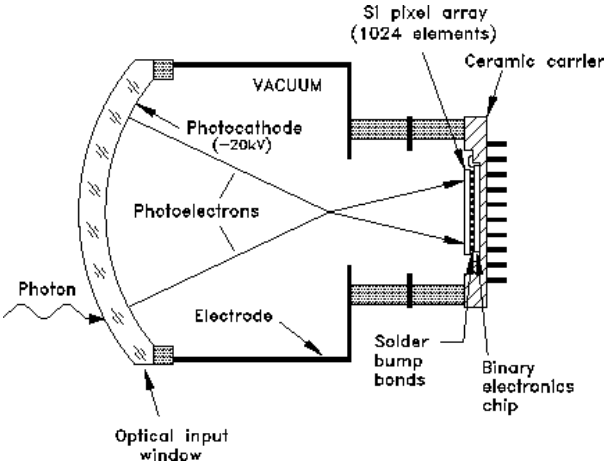

Figure 5: Schematic of the Pixel HPD, illustrating photo electron trajectories.

A schematic drawing of the HPD is shown in Figure 5. A HPD has a 7 mm thick, spherical quartz entrance window with an S20 (multialkali) photo cathode deposited on its inner surface. Its integrated quantum efficiency is $\int QdE \leq 0.7$eV. The active element of the HPD is a silicon diode sensor divided into an array of 32×32 pixels of size $0.5\,\text{mm} \times 0.5\,\text{mm}$. A cross-focusing optics provides an image demagnification of a factor of five from the photo cathode to the silicon diode sensor. The operating voltage is $-20\,\text{kV}$ at the photo cathode and the silicon sensor anode is at ground potential. The HPD is read out by a 1024 channel binary front-end chip which is encapsulated inside the vacuum envelope. The HPD has been developed together with industry.

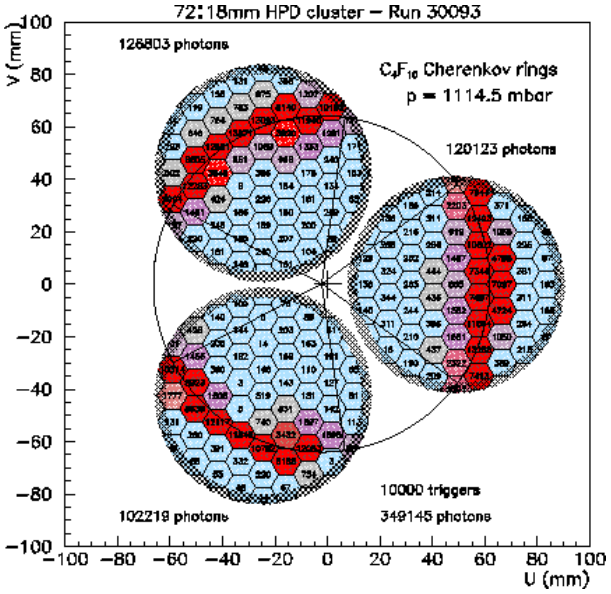

Figure 6: Display of Cherenkov photons integrated over a run for the three HPDs.

A few major results of the test programme follow. Three full scale prototype HPDs have been manufactured and were fitted with a 61-pixel silicon anode. The signals are read out externally by a Viking VA2 chip. The three 61-pixel HPDs have been mounted onto a full-scale RICH 1 prototype which was operated with a $\sim$ 1m C_4F_{10} radiator. Using the CERN SPS facility this setup has been exposed to 120 GeV/c π^- beam. This study tests the photon yield of the tube. Figure 6 displays the integrated events of a run. The Cherenkov ring is clearly visible and spans the three HPDs. The observed yield is in excellent agreement with the expectations, the figure of merit is measured to be

$202 \pm 16\text{cm}^{-1}$. The 1024 channel pixel chip provides binary output signals at LHC speed. A first design has been submitted and is currently in production. If the resulting chip were functional it will be encapsulated into the HPD. An array of 3×3 MaPMTs has also been evaluated in test beams and the measurements are in excellent agreement with the expectations. Thus the MaPMT option meets the all the performance criteria if the Pixel HPD fails to meet its milestones, although with an increased cost.

Based on the results obtained for the HPD data described above a full simulation of the RICH system has been performed. For the pattern reconstruction a global likelihood function comprising of the different particle hypotheses for all charged tracks is maximised by using all the hits in RICH 1 and RICH 2 simultaneously. The number of expected photo electrons for tracks with $\beta = 1$ is 7, 33, and 18 for the Aerogel, C_4F_{10}, and CF_4 radiator, respectively. The corresponding angular resolutions are 2.00 mrad, 1.45 mrad, and 0.58 mrad, respectively. The performance of the system is expressed as pion-kaon separation as a function of track momentum and is shown in Figure 7. This

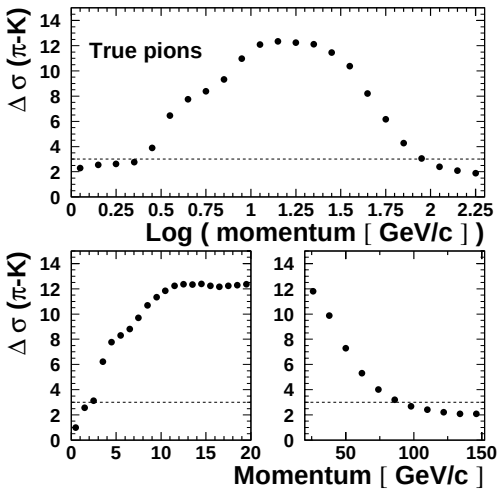

Figure 7: Pion-kaon separation for logarithmic and linear momentum scales.

demonstrates that the LHCb RICH system provides 2.5 σ or larger pion-kaon separation over the momentum range 1-150 GeV/c and 6 σ or larger separation between 3 - 60 GeV/c.

Mechanical design studies for RICH 1 and RICH 2 have been carried out. The total material of the two detectors is 14 % and 12 % of a radiation length, respectively. For RICH 1 the beam pipe is an integral part of the detector vessel and a special seal has been designed to minimize stresses to the beam pipe and to allow for bake-outs. The technical design report for the RICH system has been submitted.

4 Calorimeters

The LHCb calorimeters provide information for the Level-L0 trigger and for the reconstruction of electrons, neutral pions and photons. The electromagnetic calorimeter is of the "shashlik"-type. Lead and scintillator tiles alternate, the total thickness is 25 radiation lengths. Using wave-length shifting fibres for light collection the signals are read out by photo multiplier tubes. Keeping the number of read-out channels as a constraint it was found that the trigger and reconstruction efficiencies can be optimised by employing three different cell sizes, from 40.4 mm for the inner sections to to 121.2 mm for the outer sections. In Figure 8 we show a schematic view of a detector half. In front of the electromagnetic calorimeter there is a preshower detector consisting of a sandwich of scintillator pads - lead - pre-shower scintillators. The signals are read out by multianode photo multiplier tubes. This pre-shower provides electron-pion separation for the L0 trigger and improves upon the energy resolution. The scintillator pads allow for electron-photon separation in the L0 trigger.

The hadron calorimeter comprises of alternating iron/scintillating tiles with the tiles parallel to the beam. As in the electromagnetic calorimeter the light is collected with wave-length shifting fibres and the signals are read out by photo multiplier tubes. To facilitate the L0 trigger implementation a projective cell geometry is used for the calorimeters. For the hadron calorimeter the granularity is reduced and only two cell sizes are needed. The larger (smaller) one is twice (equal to) the projection of an outer section electromagnetic cell. This allows to construct the modules of the hadron calorimeter out of a single mechanical

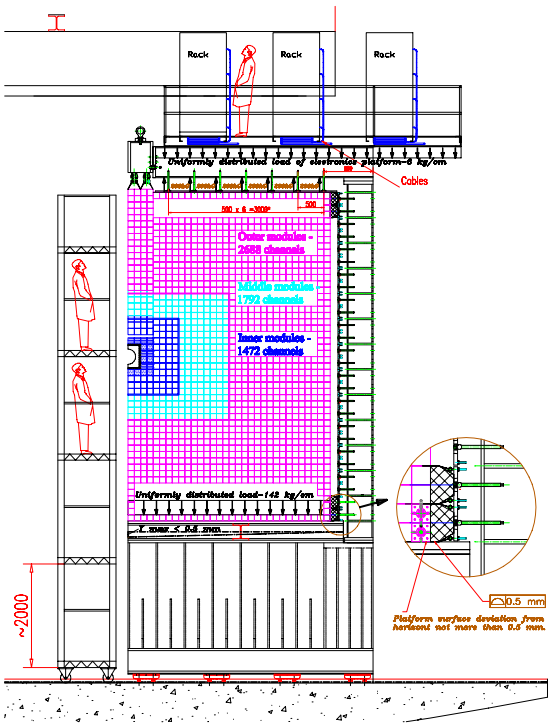

Figure 8: Front view of one half of the electromagnetic calorimeter.

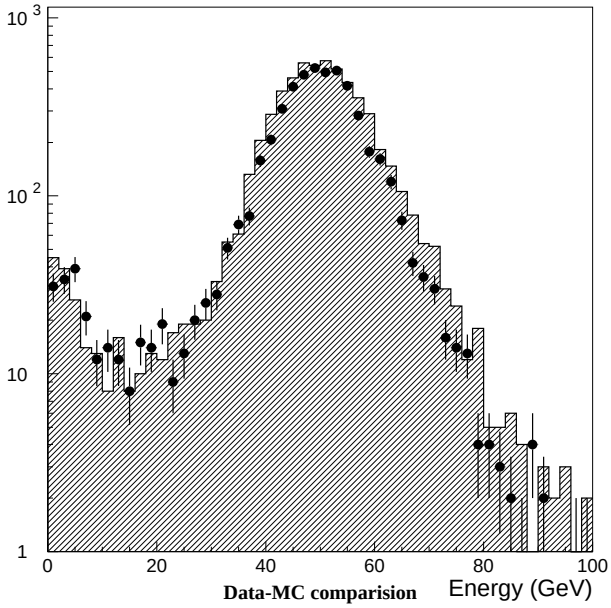

Figure 9: Energy response of a hadron calorimeter prototype for 50 GeV pions from test beam data (hatched) and and from simulation (dots).

type which reduces complexity and cost. The total thickness has been reduced from 7.3 to 5.6 nuclear interaction length. This will introduce a negligible loss of resolution.

An extensive test programme for the calorimeters has been carried out over the last few years. The design value of the energy resolution for the electromagnetic calorimeter, $\sigma_E/E = 10\%/\sqrt{E} \oplus 1.5\%$, has been obtained in measurements using prototype detectors in beam tests. The inner most electromagnetic modules have to sustain a radiation of up 0.25 Mrad/year. We have demonstrated by irradiating the scintillators and the wave-length shifters up to 5 Mrad that a subsequent annealing for 175 hours retained a total light yield such that the constant term of the resolution will not exceed the design value for more than 10 years of operation. In Figure 9 we plot the response of a hadron calorimeter module to 50 GeV pions. The test beam data agree well with the simulation which predicts an energy resolution of $\sigma_E/E = 80\%/\sqrt{E} \oplus 5\%$. The performance of the calorimeter system has also been measured by testing preshower, electromagnetic, and hadron calorimeter modules jointly. The front-end electronics board has been designed and the Technical Design Report has been submitted. Construction of the calorimeters will start in 2001.

5 Trigger

The bunch crossing frequency at the LHC is 40 MHz. The LHCb experiment will run at a tunable[3] luminosity of $2 \times 10^{32}\mathrm{cm}^{-2}\mathrm{s}^{-1}$. This relatively low luminosity optimises the number of bunch crossings with one single pp interaction, thus minimising the detector occupancies and reducing the radiation levels. It will be achieved in the first year of LHC running.

The LHCb trigger system comprises of four levels. The strategy is to have a flexible multi level

[3]The design luminosity of the LHC is $10^{34}\mathrm{cm}^{-2}\mathrm{s}^{-1}$ but by defocusing the beam optics it can be tuned to lower values at the LHCb interaction point.

trigger which does not rely on a single detector. The trigger must be stable and robust under varying conditions. A first trigger level, L0, implemented in hardware with a latency of 4μs, reduces the event rate to 1 MHz. The L0 trigger accepts events containing particles with large transverse momenta, $p_\perp$, which substantially enhances the fraction of b-quark events. Using the muon and the calorimeter systems high $p_\perp$ muons, hadrons, and electrons, photons, and neutral pions are selected.

The second trigger level is the L1 vertex trigger which must reduce the rate to 40 kHz. Taking advantage of the vertex geometry design track finding is firstly done using r-strips only. A primary vertex is reconstructed and secondary tracks are selected. Secondly the information from the φ-strips is added to select events with detached secondary vertices.

Trigger levels L2 and L3 are software based processor farms. In L2 the information from all the tracking systems is accessible whereas for L3 the full event information will be used. The data acquisition system stores events at a rate of 200 Hz. Typical trigger efficiencies are around 30 %. Simulations show that the hadron trigger is important. The tagging of the decay flavour of the B meson is based on decay products of the other B hadron: either the charge of the muons and electrons from semileptonic decays of the other B hadron or the charge of the kaons stemming from the decay chain $b \to c \to s$. The total tagging efficiency is $\varepsilon = 40\%$, the mistag rate is $w = 30\%$, leading to a effective dilution factor of $D = \varepsilon(1-2w)^2 = 6.4\%$.

6 Physics Performance

Here we describe the expected LHCb performance for a few selected channels. The trigger efficiencies, tagged event yields and LHCb sensitivities are compiled in Table 1. The excellent performance of the RICH system is demonstrated on simulated B hadrons decaying in two tracks. On the left-hand side of Figure 10 we plot the invariant mass of the two reconstructed charged tracks without particle identification. The signal for the decay mode $B^0_d \to \pi^-\pi^+$ which is sensitive to the CP violating unitarity angle α is sitting on the shoulder of the larger background mode $B^0_d \to K^-\pi^+$. Using the RICH system retains the signal with a high efficiency, whereas the background modes are eliminated or greatly reduced. This clear separation is even more important since some of the background modes can have CP violation as well. LHCb expects to reconstruct 4900 tagged signal events in one year which corresponds to a sensitivity of $\sigma_\alpha = 2 - 5^\circ$. [4]

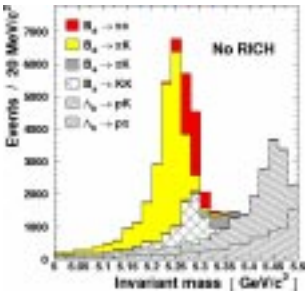

Figure 10: Mass spectrum of $B^0_d \to \pi^-\pi^+$ candidates before and after particle identification.

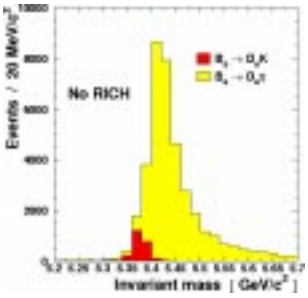

Figure 11: Mass spectrum of $B^0_s \to D^\mp_s K^\pm$ candidates before and after particle identification.

In Figure 11 we plot the invariant mass distribution for the channel $B^0_s \to D^\mp_s K^\pm$. The two charge conjugate decays are caused by two tree level diagrams which are of the same order of magnitude. Large CP violating effects are possible in the interplay of $B_s\bar{B}_s$ mixing and decay. Without particle identification the signal is dwarfed by the Cabibbo favoured mode $B^0_s \to D^\mp_s \pi^\pm$. After applying the RICH selection the signal dominates. This is crucial for measuring the four time dependent rate asymmetries which allow a determination of the unitarity angle $\gamma - 2\delta\gamma$. About 2400 tagged events

[4] This results assumes that the contribution from the penguin diagram to $B^0_d \to \pi^-\pi^+$ can be extracted separately.

are collected in one year of data taking and a measurement precision of $\sigma_{\gamma-2\delta\gamma} = 6-14^\circ$ is expected.

The decay channel $B^0_d \to \rho\pi$ is sensitive to the unitarity angle α. In Figure 12 we show a Dalitz plot for reconstructed signal events. A time dependent analysis allows to extract not only α but also the strength of both the contributing tree and penguin amplitudes. About 1300 tagged events are reconstructed in one year LHCb running yielding a sensitivity of $\sigma_\alpha = 3-6^\circ$.

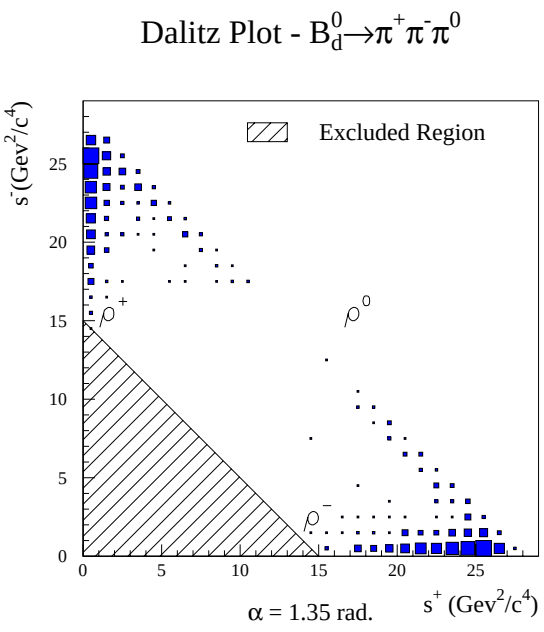

Figure 12: The Dalitz plot for $B^0_d \to \rho\pi$.

New strategies for measuring CKM angles in direct CP violation using the modes $B^0_d \to K\pi$ [9], $B^0_{d,s} \to \pi\pi, KK$ [10], and $B^0_{d,s} \to D^+_{d,s}D^-_{d,s}$ are also being developed. Complementary searches for new physics can be performed outside the unitarity triangle by searching for CP violation in channels which are expected to have very low Standard Model asymmetries. Examples are decays generated by Penguin diagrams only. LHCb has studied the sensitivity to $B^0_d \to K^{*0}\gamma$, and to $B^0_d \to K^{*0}\mu^+\mu^-$ where the forward-backward asymmetry is sensitive to contributions from MSSM models as discussed in another presentation [11]. Alternatively channels may be searched for which have extremely low, but cleanly predicted Standard Model branching ratios. For the decay $B^0_s \to \mu^+\mu^-$ the SM predicts a branching ratio of 3.7×10^{-9} and yet LHCb expects to see about 11 events of this decay within one year of data taking.

7 Conclusions

The LHCb experiment is progressing rapidly since the Technical Proposal. Major technology choices have been made. A normal conductive coil has been chosen for the magnet. The pixel HPD has been selected as the baseline photo detector for the RICH system. The Technical Design Reports for the magnet has been approved, and the TDRs have just been submitted for the RICH and calorimeters. Other subsystems such as vertex detector are well on track. Some subsystems, e.g. the calorimeters, will enter into the construction phase in early 2001. The trigger system has demonstrated its robustness and the experiment will be able to collect data from the start of the LHC. The physics performance studies have been extended and show that there will be a long and healthy physics programme for the LHCb experiment.

Acknowledgments

With great pleasure I thank my LHCb colleagues for their help in the preparation of this contribution.

References

[1] B. Hommels, in these proceedings.

[2] E. Santovetti, in these proceedings.

[3] G. Corti, in these proceedings.

[4] LHCb Technical Proposal, CERN/LHCC 98-4.

[5] LHCb Magnet Technical Design Report, CERN/LHCC 2000-7.

[6] LHCb RICH Technical Design Report, CERN/LHCC 2000-37.

Parameter	Channel	Trigger efficiency	Event yield	Sensitivity
α	$B^0_d \to \pi^+\pi^{-a}$	30%	4.9k	$2-5^\circ$
	$B^0_d \to \rho\pi$	20%	1.3k	$3-6^\circ$
$2\beta+\gamma$	$B^0_d \to D^\star\pi$	33%	340k	$>11^\circ$
β	$B^0_d \to J/\psi K^0_s$	36%	37k	0.6°
$\gamma-2\delta\gamma$	$B^0_s \to D_sK$	28%	2.4k	$6-14^\circ$
γ	$B^0_d \to D^0K^{\star 0}$	21%	0.4k	10°
$\delta\gamma$	$B^0_s \to J/\psi\phi$	38%	44k	0.6°
x_s	$B^0_s \to D_s\pi$	28%	120k	up to $x_s \sim 75$
Branching ratio	$B^0_s \to \mu^+\mu^-$	95%	11	$< 2\times10^{-9}$
	$B^0_d \to K^{\star 0}\gamma$	8%	26k	–
	$B^0_d \to K^{\star 0}\mu^+\mu^-$	–	4.5k	–

Table 1: LHCb performance for selected benchmark channels for one year of LHC operation.

[7] LHCb Calorimeters Technical Design Report, CERN/LHCC 2000-36.

[8] T. Bowcock *et al.*, at CHEP2000, Padova, 2000 and http://www.ph.liv.ac.uk/map/.

[9] G. Buchalla, in these proceedings.

[10] M. Gronau, in these proceedings.

[11] A. Ali, in these proceedings.